Geochemistry and petrogenesis of Oligocene dacites from the Central Bosnia and Herzegovina with insight in the post-collisional tectonic evolution of Central Dinaridic Ophiolite Belt

Salkić, Zehra; Babajić, Elvir; Lugović, Boško

Source / Izvornik: **Archives for Technical Sciences, 2021, 17 - 30**

Journal article, Published version
Rad u časopisu, Objavljena verzija rada (izdavačev PDF)

https://doi.org/10.7251/afts.2021.1324.017s

Original Scientific paper
UDK 546.224-31:549.755.36(497.6)
DOI: 10.7251/afts.2021.1324.017S
COBISS.RS-ID 132376065

GEOCHEMISTRY AND PETROGENESIS OF OLIGOCENE DACITES FROM THE CENTRAL BOSNIA AND HERZEGOVINA WITH INSIGHT IN THE POST-COLLISIONAL TECTONIC EVOLUTION OF CENTRAL DINARIDIC OPHIOLITE BELT

Salkić Zehra[1], Lugović Boško†[2], Babajić Elvir[1]

[1]*Faculty of Mining, Geology and Civil Enginering, University of Tuzla, Bosnia and Herzegovina,*
E-mail: salkicz@yahoo.com
[2]*Institute of Mineralogy, Petrology and Mineral Deposits; Faculty of Mining, Geology and Petroleum Engineering, University of Zagreb, Croatia*

ABSTRACT

Magmatic rocks of post-Late Eocene magmatic formation are widespread in the Sava segment of Sava-Vardar suture zone and adjoin areas. The rocks formed as a response to transpressional-transtensional tectonic activity preceded by the Cretaceous-Eocene compression of the Internal Dinarides and Tisia Unit as fragments of Eurasian continental lithosphere. Central Bosnia Tertiary volcanic rocks (CBTVR), erupted as dacites in Lower Oligocene, are peculiar rocks of this formation either by their location (southernmost distal outcrops) or geological setting (extrusive within the melange of the Internal Dinaride Ophiolite Belt).

Major element composition of the CBTVR reveals high-K calc-alkaline geochemical affinity whereas trace element discriminate the rocks as shoshonitic. The rocks are LILE-enriched and show negative Ta-Nb, P and Ti anomalies, and positive Pb anomalies typical of subduction related volcanic rocks. Chondrite-normalized REE patterns exhibit significant LREE/HREE enrichment [$(La/Yb)_{cn}$ = 21.4 - 33.4]. Geochemical affinity of the CBTVR combined with tectonic position of extrusions suggests derivation of the melts from the subcontinental mantle which had inherited strong orogenic signature during an ancient subduction.

Key words: *Oligocene, post-orogenic dacites, geochemistry, petrogenesis, Internal Dinarides*

INTRODUCTION

Dacites related to the Oligocene eruption of shoshonitic and high-K calc-alkaline volcanic rocks are common in the Central Bosnia. They occur within Tertiary magmatic formation succesivelly arising between 55 and 29 Ma in the Sava suture zone where Internal Dinarides are interfaced with the Tisia Unit of Eurasian continent. The eruptions postdate collision of northernmost Internal Dinaride tectonostratirafic units which represent a mega block of detached Europen continental lithosphere [1]. The magmatic activity is interpreted as being caused by transition from compressional tectonic regime operating in Eocene to transpressional-transtensional tectonic phase active during Early Oligocene [2].

On the basis of ages of similar magmatic formations, continuation of this post-collisional magmatism is recognized along the Periadriatic Lineament in the west [3,4,5] and in the south in the Vardar Zone [6] which prolonges to the Hellenides [7] and far away in the Taurides [8] and clearly define the Sava-Vardar-Izmir-Ankara-Erzegin suture zone.

The volcanic rocks of this formation associated with granitoids which show approximately the same age are the most common in the Sava-Vardar suture zone [9] (Figure 1). By a lesser extent these rocks are relatively also abundant in the tectonostratigraphic units located to the nord of the suture zone [2] witnessing for an active European continental margin.

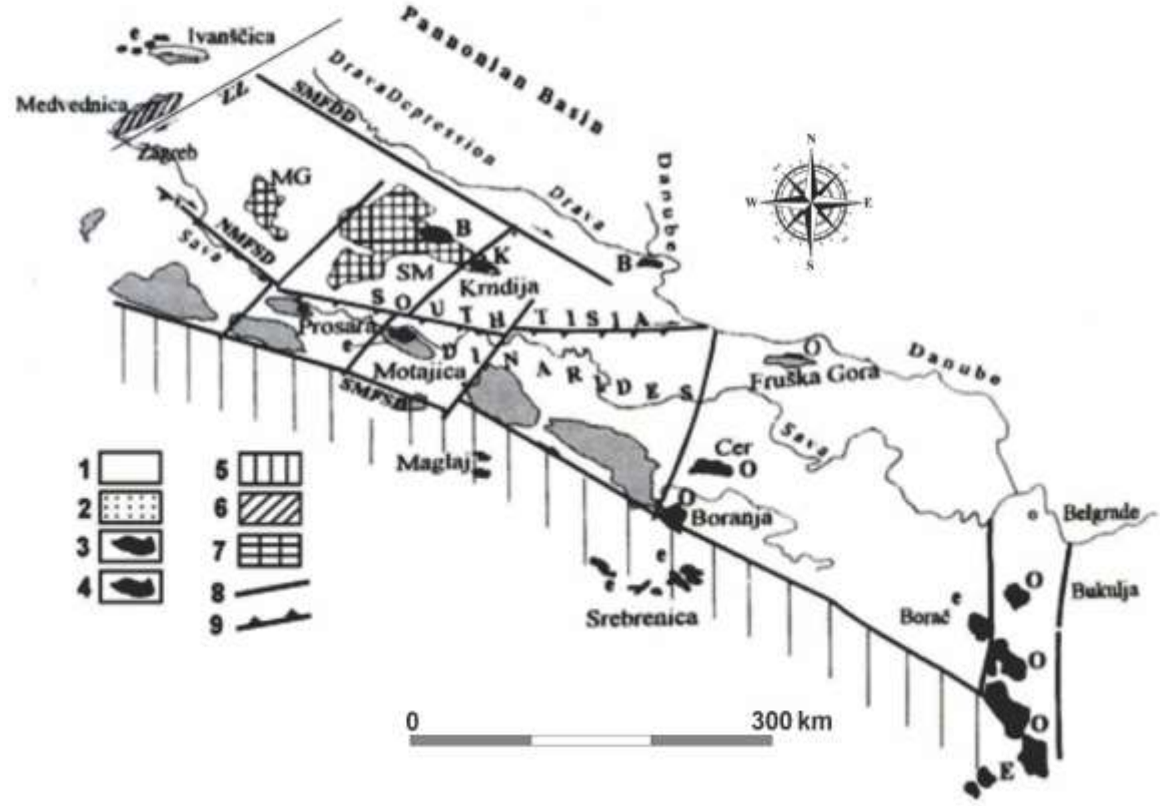

Figure 1. Position of Central Bosnian Tertiary Volcanic rocks in the frame of Periadriatic-Sava-Vardar Zone (after Pamić and Balen, 2001)

(1) Negene sedimentary fill of the Pannonian Basin; (2) Sava-Vardar Zone; (3) Tertiary granitoid formations: E - Eocene syncollisional; O - Oligocene postcollisional; ee - Egerian-Eggenburgian; (4) Tertiary volcanic formations: O - Oligocene shoshonite and calc-alkaline volcanic formations; e - Egerian-Eggenburgian calc-alkaline volcanic series: K - Karpatian shoshonites; B - Baden calc-alkaline volcanic suites; (5) Dinaride Ophiolite Zone including Paleozoic-Triassic nappes; (6) External Dinarides; (7) Pelagonide and Serbo-Macedonian Massif; (8) Sava nappe; (9) Austroalpine domain; (10) Tisian Varisciancrystalline complex; (11) fault; (12) thrust.
Large Faults: MBF - Main Balkan fault; SMFDD - Southern marginal fault of the Drava Depression: NMFSD - Nothern marginal fault of the Sava Depression; PBL - Periadriatic-Balaton; SF - Sava fault; SMFSD - Southern marginal fault of the Sava Depression; SN - Sava thrust; ZZ - Zagreb-Zemlin.
Mountains: K - Karavanke; Md - Medvednica; MG - Moslavačka Gora; P - Pohorje; SM - Slavonian MTS.

Central Bosnia dacites located far away to the south from the Sava suture zone and erupted through the different rocks of Jurassic ophiolite melange of Central Dinaride Ophiolite Zone. Bulk rock K-Ar measurement yield the ages 30.4 - 28.5 Ma which represent the oldest Tertiary post-orogenic volcanic rocks of the north Internal Dinarides [10]. Correlation of the data from the north Internal Dinarides with similar rocks from the eastern and southeastern Dinarides and North Hellenides suggest that Tertiary volcanic rocks from the Central Bosnia by location and intensity of eruption might represent the most important members of the postorogenic volcanic formations of the Sava-Vardar Zone of the Dinarides and Hellenides [11].

Central Bosnia Tertiary Volcanic Rocks (CBTVR) are situated to the south of the Sava-Vardar Suture Zone (SVSZ) intersecting the thrust sheet of Krivaja-Konjuh ophiolite underlain by genetically related ophiolite mélange of the Dinaride Ophiolite Zone (DOZ) [12]. Jurassic ophiolite mélange overstep by Lower Cretaceous Pogari Formation forms the largest part of the CBTVR. Lava extrusions are localized to several volcanic centres situated along deep faults which were a predisposition or channels for the emplacement of Tertiary magmas. Tertiary volcanic rocks of the central Bosnia are the most common in the valley of Bosna river in the area of Maglaj [13,14,15], in the vicinity of Nemila near Kolići (Kišpatić, 1904 13) and ten kilometres westward in the adjacency of Teslić [16].

Central Bosnia volcanic rocks are mostly dacites, and highly subordinately andesites as the members of the high-K calc-alkaline series. The CBTVR are plagioclase, biotite and quartz phyric with a micro- to cryptocrystalline matrix consists abundantly sanidine and quartz along with accessory amount of apatite, hematite, pseudobrookite, zircon, rutile, monazite [17].

In this paper geochemical data on representative volcanic rocks from the Central Bosnia are reported, and their genesis are discussed. Geochemical discriminant parameters were used in order to determine mantle source characteristic as a clue for interpretation of the geotectonic setting in which those rocks were emplaced.

ANALYTICAL TECHNIQUES

Eleven samples were processed in steel yaw crusher. All fragments with a weathering crust an d veins filled by secondary minerals were removed. After splitting, about 100 g were ground in an agate ring-disk mill and rock powders were dried at 110°C.

Major elements were measured on lithium borate fusion pellets by XRF using a RIX 3000 Rigaku X-ray spectrometer in the Institute MTA.

Trace elements and rare earth elements were determined by ICP-MS at the Actlab Laboratories in Ontario in Canada.

WHOLE ROCK GEOCHEMISTRY AND GEOCHEMICAL CLASSIFICATION

Chemical composition of analysed CBTVR is given in the Table 1. The rocks typically contain low FeO and MgO and high SiO_2 (60.2. - 65.5 wt.%) due to xenocrystic quartz. They are rich in alkali oxides (6.25 - 7.06 wt.%) and are potassium dominated (K_2O/Na_2O = 0.98 - 1.58). In the total alkali-silica (TAS) diagram for classification of volcanic rocks [18] all analysed samples fall in the sub-alkaline field showing dacite compositional trend (Figure 2a). In the SiO_2 versus K_2O diagram used to distinguish between volcanic rock series [19] the rocks plot in the field of high-K calc-alkaline dacites (Figure 2b). Some discrepancy between our data and these compiled from the old literature refers more likely to analytical uncertain of the latter.

Different geochemical affinity and nomenclature have arised for the CBTVR when immobile trace elements are used as discriminants. In the plot Zr/TiO_2 - Nb/Y [20] enhanced Nb relative to Y causes the rocks to plot in the field of trachyandesite (Figure 2c). In the Th/Yb–Ta/Yb the analyzed rocks fall in the field of shoshonitic rocks and after geochemical discriminant scheme of [21] applied for felsic to intermediate volcanic rocks they are akin to the volcanic rocks from active continental margins (Figure 2d).

Major and selected trace element variations of CBTVR versus SiO_2 as a discriminant are presented in the Harker type variation diagrams in Figure 3. Microscopic investigations of our samples revealed that magnetite and ilmenite were not liquidus phases and whilst zircon and rutile show similar abundance in all rocks forming weak fractional spread of Zr and Ti (see also Figure 2c). Thus, despite that quartz phenocrysts may be xenocrysts, SiO_2 was selected as the fractionation index of the CBTVR dacites rather than Zr/TiO_2 ratio utilized for similar rocks [22,23].

Table 1. Chemical composition of Central Bosnia Tertiary volcanic rocks

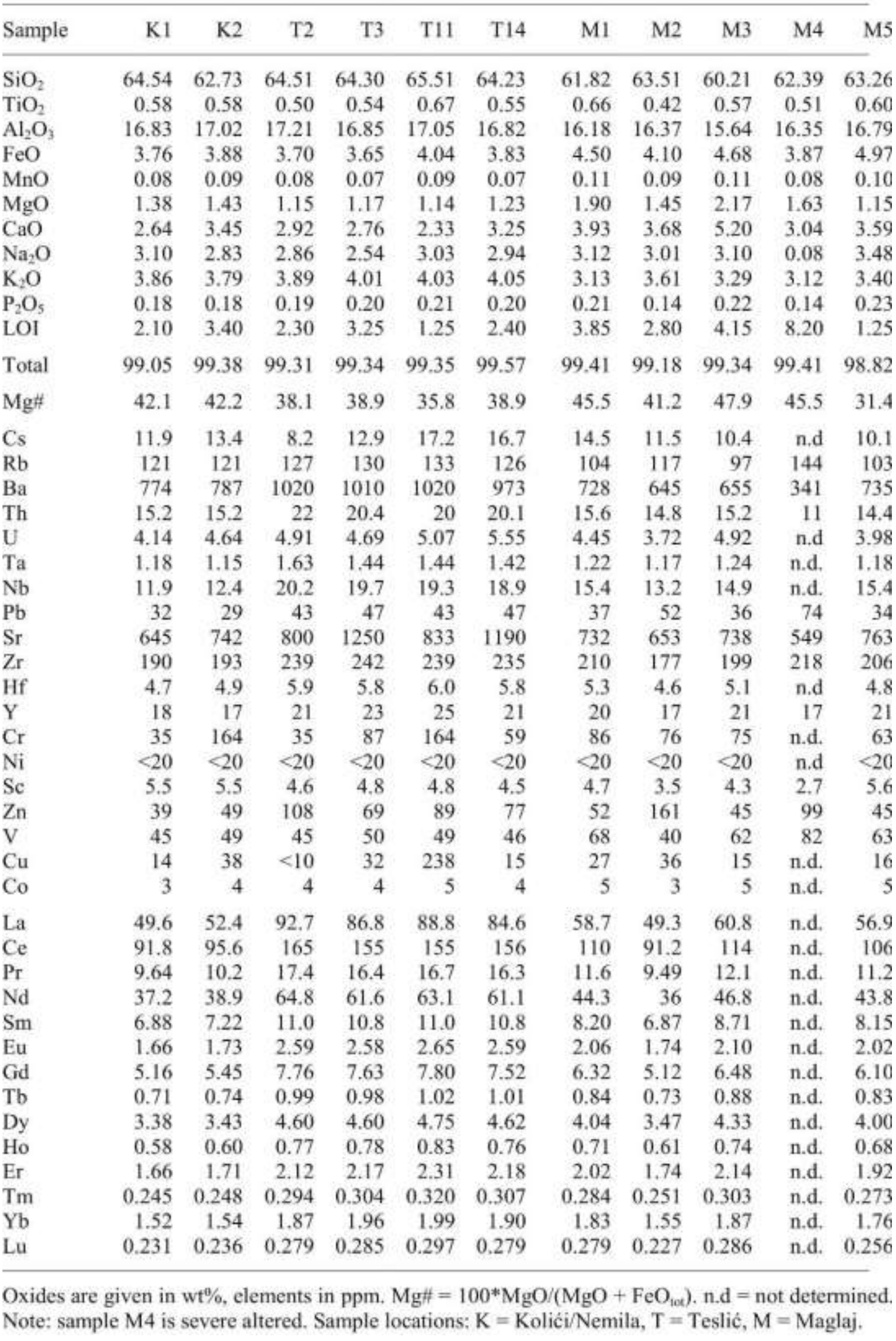

Sample	K1	K2	T2	T3	T11	T14	M1	M2	M3	M4	M5
SiO_2	64.54	62.73	64.51	64.30	65.51	64.23	61.82	63.51	60.21	62.39	63.26
TiO_2	0.58	0.58	0.50	0.54	0.67	0.55	0.66	0.42	0.57	0.51	0.60
Al_2O_3	16.83	17.02	17.21	16.85	17.05	16.82	16.18	16.37	15.64	16.35	16.79
FeO	3.76	3.88	3.70	3.65	4.04	3.83	4.50	4.10	4.68	3.87	4.97
MnO	0.08	0.09	0.08	0.07	0.09	0.07	0.11	0.09	0.11	0.08	0.10
MgO	1.38	1.43	1.15	1.17	1.14	1.23	1.90	1.45	2.17	1.63	1.15
CaO	2.64	3.45	2.92	2.76	2.33	3.25	3.93	3.68	5.20	3.04	3.59
Na_2O	3.10	2.83	2.86	2.54	3.03	2.94	3.12	3.01	3.10	0.08	3.48
K_2O	3.86	3.79	3.89	4.01	4.03	4.05	3.13	3.61	3.29	3.12	3.40
P_2O_5	0.18	0.18	0.19	0.20	0.21	0.20	0.21	0.14	0.22	0.14	0.23
LOI	2.10	3.40	2.30	3.25	1.25	2.40	3.85	2.80	4.15	8.20	1.25
Total	99.05	99.38	99.31	99.34	99.35	99.57	99.41	99.18	99.34	99.41	98.82
Mg#	42.1	42.2	38.1	38.9	35.8	38.9	45.5	41.2	47.9	45.5	31.4
Cs	11.9	13.4	8.2	12.9	17.2	16.7	14.5	11.5	10.4	n.d	10.1
Rb	121	121	127	130	133	126	104	117	97	144	103
Ba	774	787	1020	1010	1020	973	728	645	655	341	735
Th	15.2	15.2	22	20.4	20	20.1	15.6	14.8	15.2	11	14.4
U	4.14	4.64	4.91	4.69	5.07	5.55	4.45	3.72	4.92	n.d	3.98
Ta	1.18	1.15	1.63	1.44	1.44	1.42	1.22	1.17	1.24	n.d.	1.18
Nb	11.9	12.4	20.2	19.7	19.3	18.9	15.4	13.2	14.9	n.d.	15.4
Pb	32	29	43	47	43	47	37	52	36	74	34
Sr	645	742	800	1250	833	1190	732	653	738	549	763
Zr	190	193	239	242	239	235	210	177	199	218	206
Hf	4.7	4.9	5.9	5.8	6.0	5.8	5.3	4.6	5.1	n.d	4.8
Y	18	17	21	23	25	21	20	17	21	17	21
Cr	35	164	35	87	164	59	86	76	75	n.d.	63
Ni	<20	<20	<20	<20	<20	<20	<20	<20	<20	n.d	<20
Sc	5.5	5.5	4.6	4.8	4.8	4.5	4.7	3.5	4.3	2.7	5.6
Zn	39	49	108	69	89	77	52	161	45	99	45
V	45	49	45	50	49	46	68	40	62	82	63
Cu	14	38	<10	32	238	15	27	36	15	n.d.	16
Co	3	4	4	4	5	4	5	3	5	n.d.	5
La	49.6	52.4	92.7	86.8	88.8	84.6	58.7	49.3	60.8	n.d.	56.9
Ce	91.8	95.6	165	155	155	156	110	91.2	114	n.d.	106
Pr	9.64	10.2	17.4	16.4	16.7	16.3	11.6	9.49	12.1	n.d.	11.2
Nd	37.2	38.9	64.8	61.6	63.1	61.1	44.3	36	46.8	n.d.	43.8
Sm	6.88	7.22	11.0	10.8	11.0	10.8	8.20	6.87	8.71	n.d.	8.15
Eu	1.66	1.73	2.59	2.58	2.65	2.59	2.06	1.74	2.10	n.d.	2.02
Gd	5.16	5.45	7.76	7.63	7.80	7.52	6.32	5.12	6.48	n.d.	6.10
Tb	0.71	0.74	0.99	0.98	1.02	1.01	0.84	0.73	0.88	n.d.	0.83
Dy	3.38	3.43	4.60	4.60	4.75	4.62	4.04	3.47	4.33	n.d.	4.00
Ho	0.58	0.60	0.77	0.78	0.83	0.76	0.71	0.61	0.74	n.d.	0.68
Er	1.66	1.71	2.12	2.17	2.31	2.18	2.02	1.74	2.14	n.d.	1.92
Tm	0.245	0.248	0.294	0.304	0.320	0.307	0.284	0.251	0.303	n.d.	0.273
Yb	1.52	1.54	1.87	1.96	1.99	1.90	1.83	1.55	1.87	n.d.	1.76
Lu	0.231	0.236	0.279	0.285	0.297	0.279	0.279	0.227	0.286	n.d.	0.256

Oxides are given in wt%, elements in ppm. Mg# = 100*MgO/(MgO + FeO_{tot}). n.d = not determined.
Note: sample M4 is severe altered. Sample locations: K = Kolići/Nemila, T = Teslić, M = Maglaj.

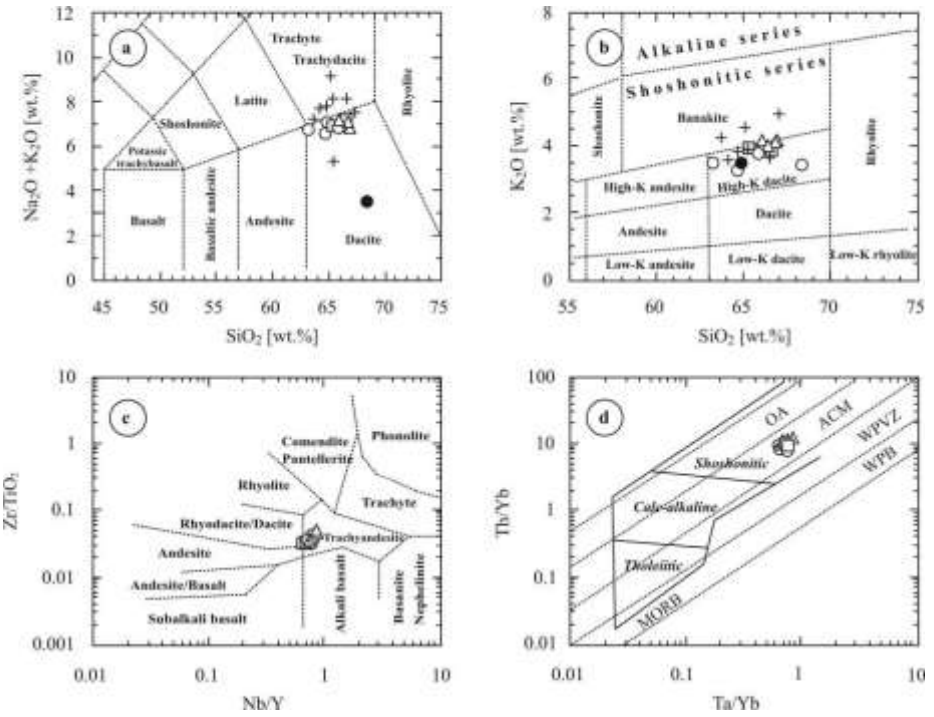

Figure 2. Systematic of geochemical classification and nomenclature of CBTVR. (a) TAS diagram [24]; (b) K_2O–SiO_2 diagram [19]; (c) Zr/TiO_2–Nb/Y diagram [20]; (d) Th/Yb–Ta/Yb diagram [25] with separating field for OA (*Oceanic arcs*), ACM (*Active continental margins*), WPVC (*Within plate volcanic zone*), MORB (*Mid-Ocean Ridge Basalts*) and WPB (*Within-plate basalts*) [21]. Symbols: squares = Kolići/Nemila, circles = Maglaj, triangles = Teslić; crosses = analyses from [14,15,16].

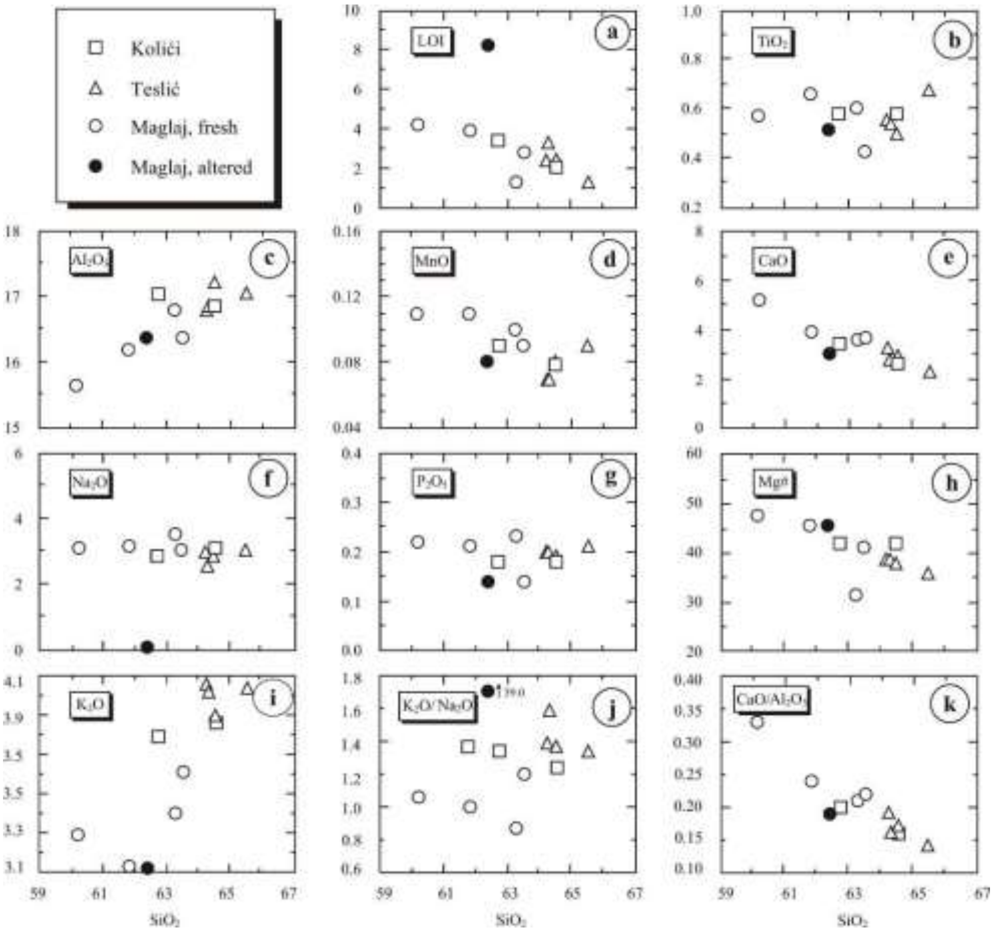

Fig. 3. Major element variations as a function of SiO_2 for CBTVR.

The Mg#, CaO and MnO decrease (Figure 3d,e and h) whilst K_2O and Al_2O_3 increase (Figure 3f and i) with increasing SiO_2. Total volatiles (LOI) form well-correlated negative trend (Figure 3a) with consequent with early fractionation of biotite and low intensity of alterations. TiO_2, Na_2O and P_2O_5 show no correlation (Figure 3b, f and g).

The CBTVR are enriched in K, Cs, Rb, Ba, Sr, Pb, Th, U, Zr, Hf, Nb, Ta, La and Y in comparison to the composition of the continental crust [26], which is characteristic of high-K magmas.

Variation diagrams of LILE: Rb, Ba and Sr (Figure 4a, b and c) increase, and HFSE: Ta, Nb, Zr, Hf and Y decrease with SiO_2 (Figure 4g, h, i, j and k).

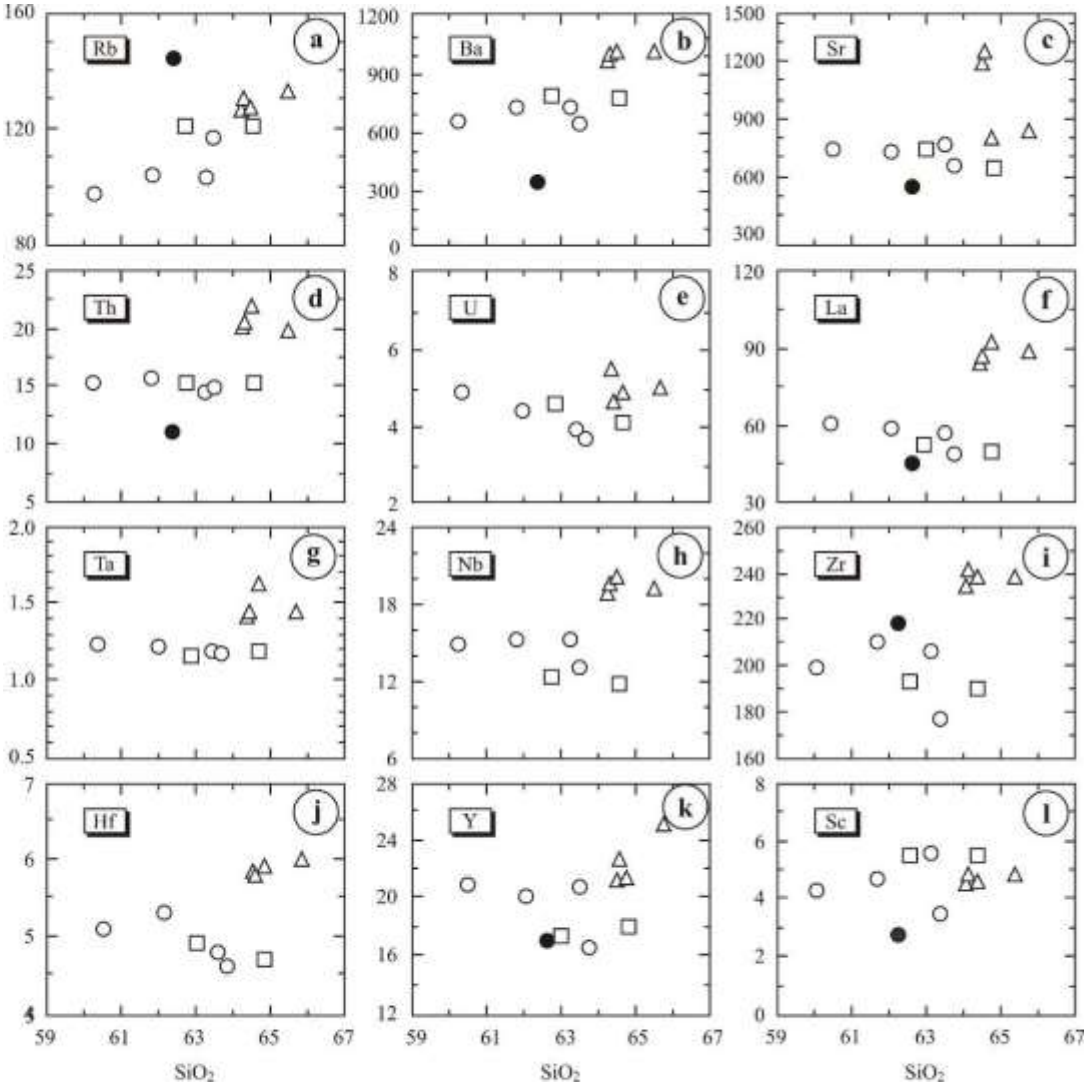

Figure 4. Trace element variations vs SiO_2 for CBTVR. Symbols as described in Figure 3.

Multi-element concentrations of the CBTVR normalized to the primitive mantle (spider diagram) are shown in Figure 5a. The rocks exhibit similar profiles and show significant enrichment of LILE (from Cs to K) and LREE (La and Ce) over all HREE and HFSE, and therefore display high negative Ta-Nb, P and Ti anomalies. All dacites show strong positive Pb anomaly.

Such geochemical patterns are distinctive for subduction-related active continental margins [27, 28] where subcontinental mantle was selectively enriched in LILE due to their high partition coefficients in the fluids extracted from subducting slab during dehydration.

Chondrite-normalized REE of the CBTVR have similar smooth profiles (Figure 10b) and exhibit strongly fractionated patterns [$(La/Lu)_n$ = 21.9 - 34.5] with flat HREE segment [$(Ho/Lu)_n$ ~ 1.1], all argue against fractionation of amphibole. All rocks have slightly negative Eu anomalies

(Eu/Eu^* = 0.85 - 0.89) suggesting that fractionation of plagioclase played an importance in evolution of the magmas.

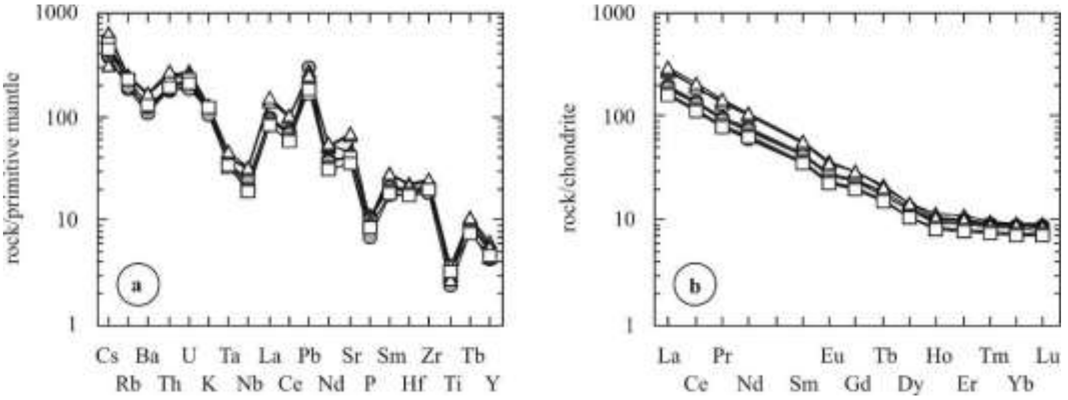

Figure 5. (a) The trace element concentrations/spider diagrams normalized the primitive mantle for CBTVR [29]. (b) Chondrite-normalized REE patterns for CBTVR [30]. Symbols as described in Figure 3.

GEOCHEMICAL GEOTECTONIC DISCRIMINATIONS

The discriminant diagrams for felsic volcanic rocks must be interpreted with caution because they were constructed for the rocks of granitic composition. The Nb–Y and Rb–(Nb+Y) discriminant diagrams [31] were used in order to geochemically compare the CBTVR with dacites from known geotectonic setting and to infer their geochemically defined setting of emplacement. On both diagrams (Figure 11a and b) rocks from both stocks plot in the Volcanic Arc Field. This caution is justified, as their location on a Rb–Hf–Ta ternary diagram [32] indicates a late/post-collisional tectonic setting; this result is consistent with the field evidence (Figure 11f). A multi-element spidergram reveals characteristic stepped profiles (Figure 10a), with values consistent with both syn- and post-collisional granites shown by [31].

Geochemical diagrams of [33] are the most appropriate for geotectonic discrimination of K-rich rocks. Discrimination fields in the diagrams are based on the ratio of selected elements for the volcanic rocks from different geotectonic settings. The diagrams utilize incompatibile and immobile elements because their ratios should closely reflect primary source differences and therefore characterize the tectonic setting of eruptions.

In the Zr/Al_2O_3 - TiO_2/Al_2O_3 discriminant diagram (Figure 6c) the CBTVR plot in the field of continental arc potassic (CAP) and post-collisional arc potassic (PAP) igneous rocks. The CAP and PAP igneous rocks are geochemically discriminated in the Ce/P_2O_5–Zr/TiO_2 (Figure 6d) and Nb*50 - Zr*3 - Ce/P_2O_5 (Figure 6e). On the both diagrams analyzed rocks plot in the field of CAP igneous rocks from orogenic continental margin regions indicative for the rocks related to Andean type of subduction.

Geochemical diagrams, used in order to determine the geotectonic setting in which the rocks were emplaced show typical subduction-related volcanic-arc characteristics which is in strongly discrapance with the field evidence. The field data for the volcanic activity generated the rocks have occurred in post-orogenic phase, that is, in transpressional and extensional conditions [2]. However, CAP and PAP geotectonic settings successive involve destruction and consummation of oceanic crust in a subductional and collisional setting, they not unexpectedly generate potassic volcanic rocks of similar composition, and therefore geochemical overlaps are unvoidable.

FRACTIONAL CRYSTALLIZATION

I the most Harker variation diagrams the CBTVR display linear variation trends (Figure 3). The major and trace element variations are consistent with fractionation of the observed phenocrystic plagioclase, biotite, sanidine and quartz.

Amount of $Na_2O + K_2O$ increase (Figure 3j), while the CaO/Al_2O_3 ratio decrease with increasing SiO_2 (Figure 3k), confirming that feldspar fractionation has been an important process controlling major element variations. Positive correlation between K and Rb in the CBTVR (not presented in this paper) suggests that they are highly enriched in the residual liquid and it is consistent with the crystal-liquid fractionation-dominated processes.

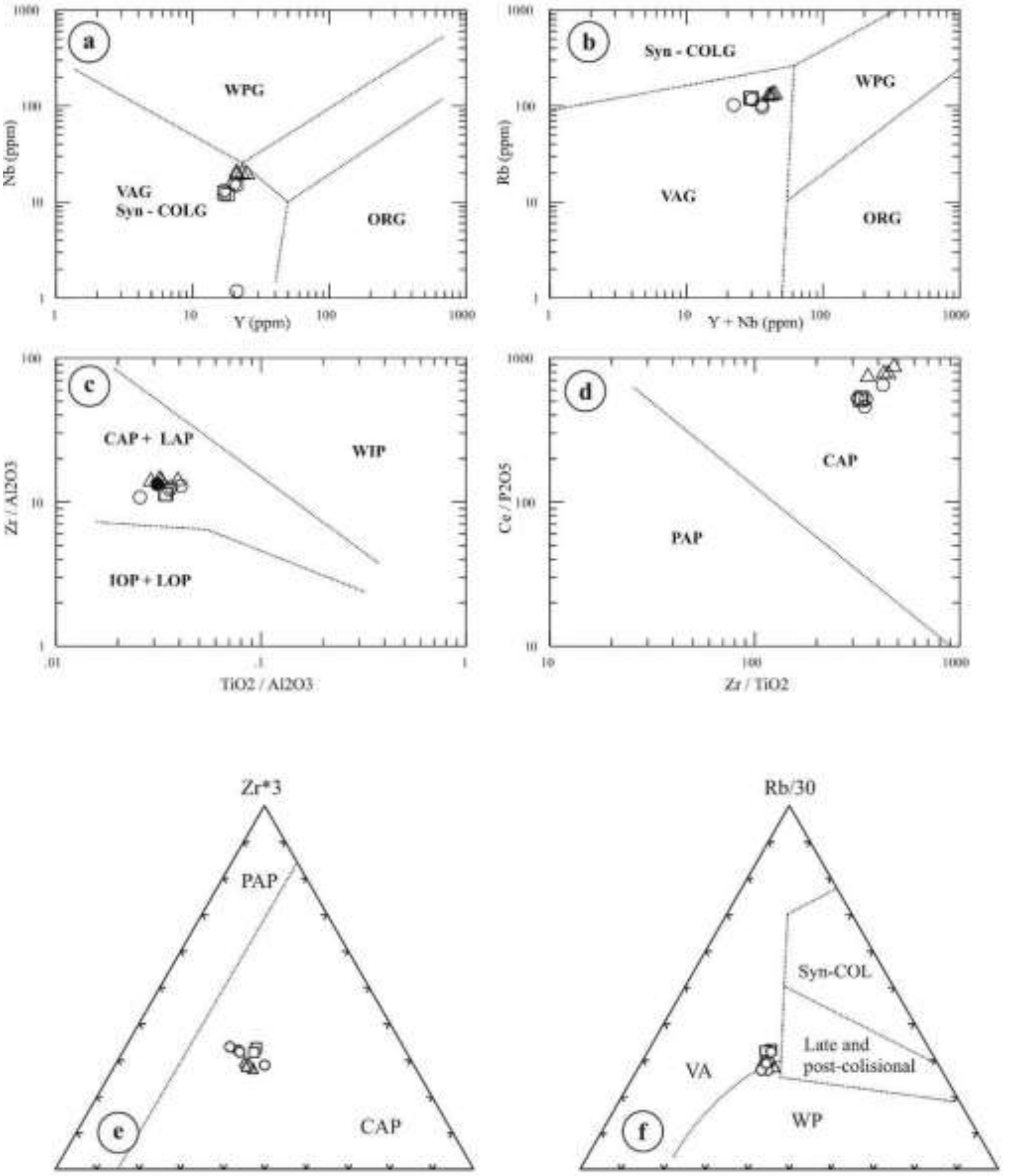

Figure 6. Diagrams illustrating tectonic setting of magmatism: (a) Nb–Y [31]; (b) Rb–(Y+Nb) [31]; (c) Zr/Al_2O_3–TiO_2/Al_2O_3 [33]; (d) Ce/P_2O_5–Zr/TiO_2 [33]; (e) Nb*50–Zr*3–Ce/P_2O_5 [33]; (f) and Rb–Hf–Ta [34]. Symbols as described in Figure 3.

Decreasing La with increasing SiO_2 is indicated by fractionation of monacite (Figure 4f).
Relatively low abundance of Y and Yb, as well as the negative correlation Y with SiO_2 (Figure 4k) confirm the fractionation of pyroxene and amphibole. Low Sc content (2.7 - 5.5) can be due to early fractionation of clinopyroxene.

The concentrations of Ba, Sr, Th, La, Ta, Nb, Zr, Hf and Y in the dacites from Teslić are higher than in Maglaj and Kolići rocks, and in trace element variations diagrams these dacites form a separate group (Figure 4d, g, h, f, i, j and k). This can indicate that the dacites from Teslić represent the separate petrogenetic unit.

The combination of relatively high $(La/Yb)_n$ and low $(Tb/Yb)_n$ (21.4 - 33.4 and 2.0 - 2.3, respectively) could be explained by moderate fractionation of amphibole, zircon, apatite and monacite. Significant negative Ti and P anomalies in spider diagrams are consistent with crystallization of magnetite, ilmenite, rutile, monacite and apatite (Figure 5a).

Microscopic observations show that zircon becomes more abundant than magnetite and ilmenite as the igneous rocks become more evolved. Decreasing Zr and Hf abundances with increasing SiO_2 point to fractionation of zircon as an accessory mineral (Figure 4i and j). Also Zr/Y and Hf/Lu values (9.5 - 11.2 and 17.8 - 21.2, respectively) which increase with increasing SiO_2, argue against significant fractionation of aphibole and zircon in the volcanic rocks of the central Bosnia (Figure 7g and m). The $(Tb/Yb)_n$ value which stays approximately constant with increasing SiO_2 (Figure 7p) support this view.

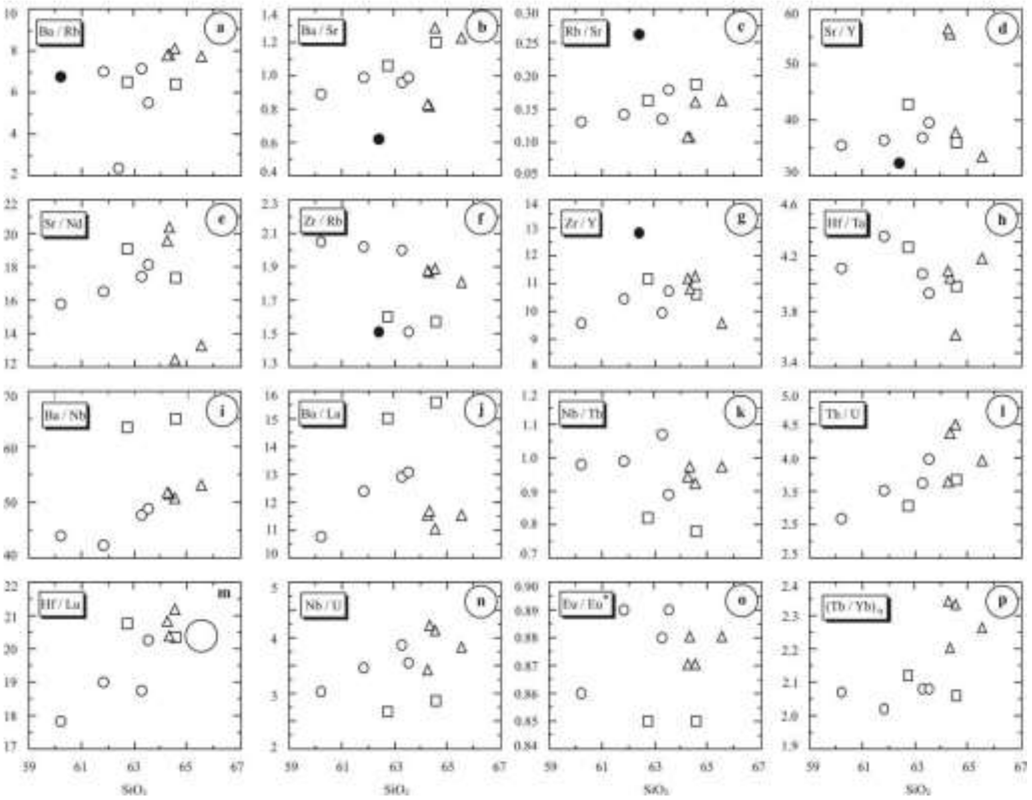

Figure 7. Variation of element ratios with SiO_2 for CBTVR. Symbols as described in Figure 3.

The incompatibile trace element ratios such as Ba/Rb, Ba/Sr and Rb/Sr increase with increasing SiO_2 that is suggest on crystal fractionation processes (Figure 7a, b and c).

CRUSTAL CONTAMINATION AND AFC PROCESSES

Certain scatter in some graphs cannot be explained by simple crystal fractionation from a common parent magma. More likely, such variations are effected by variable contribution and assimilation of upper continental crust within the magmas chamber AFC.

Increase of K_2O/Na_2O values with increasing SiO_2 is probably caused by assimilation of continental crust rocks which are enriched in potassium (Figure 3j).

A very significant enrichment in Ba, Rb and Sr indicate that the magma, generating the CBTVR may have be contaminated by crustal material. High abundance of Sr and the variations in Sr contents (645 - 1.250 ppm) are evidences that plagoclase fractionation was not dominant and exclusive process during evolution of the magmas.

Analyzed rocks have a slight negative Eu anomaly (Eu/Eu* = 0.85 - 0.89) and do not show any conspicuous correlation between their Eu/Eu* values and SiO_2 (Figure 7) suggesting that plagioclase fractionation was of relatively minor importance during genesis of the rocks and point to the AFC processes. The Sr/Y ratio which is not correlated with SiO_2, and Sr/Nd values which are positively correlated with SiO_2 confirm that fractionation of plagioclase was of minor importance (Figure 7d and e).

Hf/Ta (3.6 - 4.3) and Zr/Rb (1.5 - 2.1) ratios are generally low reflecting crustal contamination, i.e. a crustal contribution of Rb- and Ta-enriched crustal material to the magmas during their ascent. Relatively high Ba/Nb (44 - 65) and Ba/La (10.8 - 15.6) as well as relatively low Nb/Th (0.78 - 1.07) support a substantial involvement of material from the continental crust.

The CBTVR have relatively low abundance of U (3.72 - 5.55 ppm) and relatively high Nb/U (2.7 - 4.2) and Th/U (3.1 - 4.5) values which are positively correlated with SiO_2 (Figure 7n and l). Such ratios suggest decreasing assimilation of crustal material with differentiation. Also the small trough at Nb observed in the spider diagram patterns may indicate contamination the CBTVR magmas by addition of crustal material (Figure 5a). The variations of the ratios such as Hf/Ta, Zr/Rb, Ba/Nb, Ba/La and Nb/Th with SiO_2 (Figure 12h, f, i, and k) also suggest that magma composition changed by AFC processes.

Petrographic and trace element evidence demonstrates that magma mixing preceded the eruption of CBTVR. The presence of a resorbed rim enclosed the coexisting quartz phenocrysts can be interpreted by mixing of magmas with different temperatures and composition.

The flow contains reversely zoned plagioclase phenocrysts and biotite and pseudomorphs composed of silicates and opaque oxides. Partially resorbed quartz grains are also present. Plagioclase phenocrysts are assumed to record fractionation-assimilation events in different parts of the magma chamber. Early formed plagioclase phenocrysts crystallized under AFC conditions close to the roof of the chamber and were subsequently entrained in a liquid mixture composed of evolved interstitial liquid held in the partly crystallized roof zone and newly injected parental magma [35].

PHENOCRYST DISEQUILIBRIUM AND EVIDENCE OF MAGMA MIXING

Changes of the physical and chemical conditions during crystallization may significantly affect original melt composition through a variety of acting processes. These changes are ordinary revealed from the compositional and microtextural unconformity of phenocrysts which record abrupt changes related to decompression during fractional crystallization [36,37] or magma mixing and mingling through self-mixing processes in a magma chamber [38] or by input and interaction of a magma from an external source [39,8,40].

Plagioclase disequilibrium textures in the CBTVR are recorded by zoning combined with sieve-textures of large phenocrysts [17]. These fenomena are interpreted as results of heating above the existing plagioclase liquidus by mixing with a hotter magma [41,42,43] which causes solution and change to more calcic composition of sieved zone compared to the previous zone of exposed plagioclase [44] or to at least similar composition to the matrix plagioclases [39].

Sieve texture may also form as a result of rapid adiabatic decompresion (i.e. changes in intensive parameters such as fH_2O or pressure) during magma ascent towards the surface. In this case sieve-textured zone is not followed by compositional change in subsequent clear zone [36], which means that a different explanation: the mixing evolved (trachydacitic?) cooler magma with small amount of mafic magma more liable. No individual eruptions of mafic magmas.

Pseudomorph after biotite consisting of fine-grained oxides and silicates [17]. Similar reaction products of biotite in dacites were interpreted by [43] as resulting from dehydration above its stability limit attending magma mixing. Another disequilibrium feature is the development of a reaction rim on biotites. This phase can be replaced by Fe–Ti oxides with increasing reaction, and pseudomorphs after and biotite are common [17]. Reaction rims on mafic phases indicate that the water content in the magma became too low for these hydrous minerals to be stable. Two alternative explanations are viable for the reverse zoning in biotite crystals: either increasing magmatic H_2O caused the phases to precipitate more Mg-rich rims in order to reach equilibrium, or more mafic magma invaded the magma chamber [45,46].

Large quartz phenocrysts are corroded and embayed (resorption textures) indicate disequilibrium with coexisting magma [17]. Such features suggest they are xenocrystals entrained into the magma from crustal rocks From the textural viewpoint we explain quartz as xenocrystal entrained in basaltic magma (disequilibrium texture) during its ascend, before mixing with felsic magma. Growth quartz-sanidine coronas on quartz (Figure 4a) can be explained by diffusion in a boundary layer surrounding quartz according to [48].

Magma mixing or mingling is one of the significant processes in the evolution of magmas. The term mixing [48] is applied when the magmas have a homogeneous composition, whereas the term mingling is used if the magmas are mixed physically but heterogeneously, with banding or enclaves/inclusions present.

From the petrographic and chemical characteristics it is obvious that magma mixing and mingling played significant role in the evolution of the CBTVR. Petrographic evidences (disequilibrium textures) are: sieved or dusty plagioclase rim; normal and sieved plagioclase in the same sample; rounded and embayed quartz; reaction rim on biotite and pseudomorphs after mafic phases [17].

SOURCE REGION CHARACTERISTICS

Records of the tectonic evolution of the Central Bosnia indicate that the Oligocene volcanism formed in a post-collision setting following the southwest vergent intraoceanic obduction which ended by suture/collision between the Adriatic and Eurasian continental lithosphere in the Tisia sector.

For the postcollisional calc-alkaline and shoshonitic magmas, two possible options to explain enrichment in LILE and LREE relative to HFSE are: (1) a subduction component inherited from earlier subduction events or (2) crustal contamination through assimilation and fractional crystallisation (AFC) and/or MASH (melting, assimilation, storage and homogenisation).

Major and trace element concentrations indicate that the CBTVR have similar composition to the dacite-rhyolite associations orogenic continental margin regions in the western (Andean) South America and the southwest Pacific [49,50,51].

Spider diagrams for the CBTVR (Figure 5a) show significant enrichment in LILE such as K, Rb and Ba over the HFSE. There is an overall decrease in abundance from the most to the least incompatible elements which is characteristic of all subduction-related high-K volcanic suite [50] and of the volcanic rocks generated in (post)collisional zones. LILE are important components of the continental crust and they also may be useful indicators for crustal contamination of magmas which have originated in the mantle.

The CBTVR show high enrichment in LREE over the HREE, and slight negative Eu anomaly (Figure 5b) which is typical for the volcanic rocks generated by fractional crystalization from the magmas that derived from the metasomatized subcontinental mantle wedge in subductional- collisional regime.
Significant enrichment of the CBTVR in LILE and LREE clearly point to conclusion that primary magmas, in general, originate from the metasomatized segment of the upper mantle. The absence of garnet in the source region suggests that deeper part of upper mantle were not affected by partial melting.

Cs abundance ranges between 8.2 and 17.2 ppm what is characteristic of all volcanic rocks generated in orogenic zones [52]. The K/Rb values, ranging from 250 to 282, are generally high and similar to those of average continental crust (about 250) [53] and characteristic of calc-alkaline volcanics rocks generated in continental margin regions.

FSE are commonly depleted and LILE become enriched in the upper mantle (WEDGE) as a result of previous metasomatism [54]. Thus, high LILE/HFSE ratios (K/Ti, K/Zr, K/Nb and Ba/Nb) and negative HFSE anomalies in the CBTVR can be considered as result of compound processes in the magmatic system which derived from the mantle wedge. It is necessary to emphasize that such characteristics need not be in connection with simultaneous subduction, but the characteristics can be inherited from an ancient subduction. Because of that the magmatic activity in distinctly extensional regime can have subduction (orogenic) geochemical characteristics.

CONCLUSION

Spider diagrams for the CBTVR show significant enrichment in LILE such as K, Rb and Ba over the HFSE. There is an overall decrease in abundance from the most to the least incompatible elements which is characteristic of all subduction-related high-K volcanic suite and of the volcanic rocks generated in (post)collisional zones.

The CBTVR show high enrichment in LREE over the HREE, and slight negative Eu anomaly which is typical for the volcanic rocks generated by fractional crystalization from the magmas that derived from the metasomatized subcontinental mantle wedge in subductional- collisional regime.

The geochemical parameters of the central Bosnia Oligocene volcanic rocks are strong akin to subductional related volcanic rocks of Andean type of subduction although the magmas crystallized the dacites generated in transpressional-transtensional tectonic setting during Lower Oligocene, long after the subduction ceased.

Discrepance between geochemical and field evidence about geotectonic setting of the eruptions can be explained by different composition of the mantle beneath the Dinaridic Ophiolite Zone and the Sava-Vardar Zone. The overal geochemical characteristic of the dacites suggest that the subduction affinity in the mantle was inrited and extended by input of crustal materials, and also, that the manlte beneath Central Dinaridic Ophiolite Zone has different characteristics compared to the mantle of the Sava-Vardar Zone being less extensively metasomatized by subduction of the Tethyan Mesozoic oceanic lithosphere.

Received January 2021, accepted February 2021)

REFERENCE

[1] Pamić, J., Balen, D. and Herak, M. (2002). Origin and geodynamic evolution of Late Paleogene magmatic associations along Periadriatic-Sava-Vardar magmatic belt. *Geodinamica Acta* 15, 209-231.

[2] Pamić, J. and Balen, D. (2001). Tertiary magmatism of the Dinarides and the adjoing South Pannonian Basin: an overview. *Acta Vulcanologica* 13, 9-24.

[3] Altherr, R., Lugović, B., Meyer, H.-P. and Majer, V. (1995). Early Miocene post-collisional calc-alkaline magmatism along the easternmost segment of the Periadriatic fault system (Slovenia and Croatia). Mineralogy and Petrology 54, 225-247.

[4] Slapansky, P., Belocky R., Fröschl H., Hradecky P. and Spindler S.P. (1999). Petrographie, Geochemie und Einstufung des Miozänen Vulkanismus im Steirischen Becken (Österreich). Abh. *Geol. B.-A. Wien* 6/1, 419-434.

[5] Boev, B. and Yane, Y. (2001). Tertiary magmatism within the Republic of Macedonia: a review. *Acta Vulcanologica* 13, 57-71.

[6] Eleftheriadis, G., Christofides, G. Mavroudchiev, B., Nedyalkov, R., Andreev, A. and Hristov, L. (1989). Tertiary volcanics from the East Rhodope in Greece and Bulgaria. *Geol. Rhodop.* 1, 280-289.

[7] Bozkurt, E., Koçyiğit, A., Winchester, A.J., Holland, G. and Beyhan, A. (1999). Petrochemistry of the Oyaca-Kedikayasi (Ankara) dacites as evidence for the post-collisional tectonic evolution of north-cantral Anatolia, Turkey. *Geological Journal* 34, 223-231.

[8] Yurtmen, S. and Rowbotham, G. (2002). Geochemistry, mineralogy and petrogenesis of the northeast Niğde volcanics, central Anatolia, Turkey. *Geological Journal* 37, 189-215.

[9] Boev, B., Lepitkova, S. and Bermanec, V. (2000). Tertiary volcanic activity in the Inner Dinarides (Republic of Macedonia). *Vijesti hrvatskog geološkog društva* 37, 26-28.

[10] Pamić, J., Pécskay, Z. and Balen, D. (2000). Lower Oligocene K-Ar ages of high-K calc-alkaline and shoshonite rocks from North Dinarides in Bosnia. *Mineralogy and Petrology* 70, 313-320.
Pearce, J. A. (1982). Trace element characteristics of lavas from destructive plate boundaries. *In*: Thorpe, R.S. (ed), *Andesites: Orogenic Andesites and Related Rocks*. Wiley, Chichester, 525–548.

[11] Balen, D. and Pamić, J. (2001). Tertiary shoshonite volcanic associations from the adjoining area of the South Pannonian Basin and Dinarides. Acta Vulcan., 113(1-2), 117-125.

[12] Trubelja, F. (1978). Tercijarni magmatizam. Geologija BiH, knjiga IV, Magmatizam i metalogenija, Sarajevo, 219-235.

[13] Kišpatić, M. (1904). Andeziti i daciti uz obalu Bosne. *Rad JAZU* 159, 28-38.

[14] Trubelja, F. and Pamić, J. (1956). Novi prilog poznavanju dacitskih stijena okolice Maglaja. *Geološki glasnik* XX, 59-66.

[15] Pamić, J., Dimitrov, P. and Zec, F. (1964). Geološke karakteristike dacitoandezita u dolini Bosne. *Geološki glasnik* X, 241-250.

[16] Majer, V. (1961). Dacitoid iz potoka Blatnica kod Teslića u Bosni. *Vesnik* 19, 235-239.

[17] Salkic, Z., Lugovic, B. and Babajic, E. (2020): Petrography and mineral chemistry of oligocene shoshonitic dacites from the central Bosnia. Archives for Technical Sciences 2020, No.22., Technical Institute of Bijeljina, 1-10.

[18] LeBas, M.J., Le Maitre, R.W., Streckeisen, A. and Zanettin, B. (1986). A chemical classification of volcanic roks based on the total alkali-silica diagram. *Mineralogy and Petrology* 27, 745-750.

[19] Peccerillo, A. and Taylor, S.R. (1976). Geochemistry of Eocene calc-alkaline volcanic rocks from the Kastamonu area, Northern Turkey. *Contribution to Mineralogy and Petrology* 58, 63-81.

[20] Winchester, J. A. and Floyd, P.A. (1977). Geochemical discrimination of different magma series and their differentiation products using immobile elements. *Chemical Geology* 20, 325-343.

[21] Gorton, M. P. and Schandl, E.S. (2000). From continents to island arcs: a geochemical index of tectonic setting for arc-related and within-plate felsic and intermediate volcanic rocks. *The Canadian Mineralogist* 38, 1065-1073.

[22] Watson, E. B. and Harrison, T. M. (1983). Zircon saturation revisited: Temperature and compositional effects in a variety of crustal magma types. *Earth and Planetary Science Letters* 64, 295–304.

[23] Green, T. H. and Pearson, N. J. (1986). Ti-rich accesory phase saturation in hydrous mafic-felsic compositions at high P, T. *Chemical Geology* 54, 185–201.

[24] Le Bas, M. J., Le Maitre, R.W., Streckeisen, A. and Zanettin, B. (1986). A chemical classification of volcanic roks based on the total alkali-silica diagram. *Mineralogy and Petrology* 27, 745-750.

[25] Pearce, J. A. (1983). The role of sub-continental lithosphere in magma genesis at active continental margins. *In*: Hawkesworth, C. J., Norry, M. J. (eds), *Continental Basalts and Mantle Xenoliths*. Shiva Geology Series, Cheshire, UK, 230-249.

[26] Taylor, H. P. and McLennan, SM. (1985). The continental crust: its composition and evolution. Blackwell, Oxford, 312.

[27] Pearce, J. A. (1982). Trace element characteristics of lavas from destructive plate boundaries. *In*: Thorpe, R.S. (ed), *Andesites: Orogenic Andesites and Related Rocks*. Wiley, Chichester, 525–548.

[28] Pearce, J. A. (1983). The role of sub-continental lithosphere in magma genesis at active continental margins. *In*: Hawkesworth, C. J., Norry, M. J. (eds), *Continental Basalts and Mantle Xenoliths*. Shiva Geology Series, Cheshire, UK, 230-249.

[29] Hofmann, A. (1988). Chemical differentiation of the Earth: The relationship between mantle, continental crust, and oceanic crust. *Earth and Planetary Science Letters* 90, 297–314.

[30] Boyton, W.V. (1984). Cosmochemistry of the rare earth elements: Meteorite studies. In: Henderson, P. (ed.). Rare Earth Element Geochemistry. Elsevier, 63-107.

[31] Pearce, J. A., Harris, N. B. W. and Tindle, A. G. (1984). Trace element discrimination diagrams for the tectonic interpretation of granitic rocks. Journal of Petrology 25, 956-983.

[32] Harris, N. B. W., Pearce, J. A. and Tindle, A. G. (1986). Geochemical characteristics of collision-zone magmatism. In:Coward, M.P. and Ries, A.C. (eds.). Collision Tectonics. Special Publications 19. Geological Society, London, 67-81.

[33] Müller, D., Stumpfly, E. F. and Taylor, W. R. (1992). Shoshonitic and alkaline lamprophyres with elevated Au and PGE concentrations from the Kreuzeck Mountains, Eastern Alps, Austria. Mineral Petrol 46:23-42.

[34] Harris, N. B. W., Pearce, J. A. and Tindle, A. G. (1986). Geochemical characteristics of collision-zone magmatism. In:Coward, M.P. and Ries, A.C. (eds.). Collision Tectonics. Special Publications 19. Geological Society, London, 67-81.

[35] Mazzone, P. and Grant, Norman, K. (1988). Mineralogical and isotopic evidence for phenocryst-matrix disequilibrium in the Garner Mountain andesite. Contributions to Mineralogy and Petrology 99, 267 – 272.

[36] Nelson, S. T. and Montana, A. (1992). Sieve-textured plagioclase in volcanic rocks produced by rapid decompression. *American Mineralogist* 77, 1242-1249.

[37] Cashman, K., and Blundy, J. (2000). Degassing and crystallization of ascending andesite and dacite. *Philosophical Transactions of the Royal Society of London* A 358, 1487-1513.

[38] Couch, S., Sparks, R. S. J. and Caroll, M. R. (2001). Mineral disequilibrium in lavas explained by convective self-mixing in open magma chambers. *Nature* 411, 1037-1039.

[39] Mišković, A. and Francis, D. (2006). Interaction betwen mantle-derived and crustal calc-alkaline magmas in the petrogenesis of the Paleocene Sifton Range volcanic complex, Yukon, Canada, 104-134.

[40] Ishizaki, Y. (2007). Dacite-basalt magma interaction at Yakedake volcano, central Japan: petrographic and chemical evidence from the 2300 years B.P. Nakao pyroclastic flow deposits. *Journal of Mineralogicaland Petrological Sciences* 102, 194-210.

[41] Anderson, A. T. (1976). Magma mixing: Petrologic process and volcanological tool. *Journal of Volcanology and Geothermal Research* 1, 3-33.

[42] Tsuchiyama, A. (1985). Dissolution kinetics of plagioclase in the melt system diopside-albite-anorthite, and origin of dusty plagioclase in andesites. *Contribution to Mineralogy and Petrology* 89, 1-16.

[43] Nixon, G. T. (1988). Petrology of younger andesites and dacites of Iztaccihuatl volcano, Mexico: disequilibrium phenocryst asemblages as indicators of magma chamber processes. *Journal of Petrology* 29, 213-264.

[44] Stimac, J. A. and Pearce, T. H. (1992). Textural evidence of mafic–felsic magma interaction in dacite lavas, Clear Lake, California. *American Mineralogist* 77, 795–809.

[45] Luhr, J. F. and Carmichael, I. S. E. (1980). The Colima volcanic complex, Mexico: I. Post-caldera andesites from volcano Colima. Contrib. Mineral. Petrol. 71, 343–372.

[46] Halsor, S. P. and Rose, W. I. (1991). Mineralogical relations and magma mixing in calc-alkaline andesites from Lake Atitlan, Guatemala. Mineral. Petrol. 45, 47–67.]

[47] Sato, H. (1975). Diffusion coronas around quartz xenocrysts in andesites and basalts from Tertiary volcanic region in northeastern Shikoku, Japan. Contributions to Mineralogy and Petrology, 50, 40-64.

[48] Sparks, R. S. J. and Marshall, A. (1986). Thermal and mechanical constraints on mixing between mafic and silicic magmas. Journal of Volcanology and Geothermal Research, v.29, 99-124.

[49] Ewart, A. (1979). A rewiev of the mineralogy and chemistry of Tertiary-Recent dacitic, latitic, rhyolitic, and related salic volcanic rocks. In Trondhjemites, Dacites,, and Related Rocks, Barker F (ed.). Elsevier: Amsterdam; 13-121.

[50] Ewart, A. (1982). The Mineralogy and Petrology of Tertiary-Recent Orogenic Volcanic Rocks: with special reference to the andesitic-basaltic compositional range. In: THORPE RS (Ed), Andesites, New York, J Wiley & Sons, p. 25-87.

[51] Price. R. S., Stewart, R. B., Woodhead, J. D. and Smith, I. E. M. (1999). Petrogenesis of high-K Arc magmas: evidence from Egmont volcano, North Island, New Zeland. Journal of Petrology 40: 167-197.

[52] Gill, J. B. (1981). Orogenic andesites and plate tectonics. Mineral & Rocks, 16. Springer Verlag, Berlin-Heidelberg-New York. 390 pp.

[53] Jakeš, P. and White, A. J. R. (1970). K/Rb ratio of rocks from island arcs. Geochimica et Cosmochimica Acta 34, 849-856.

[54] Hole, M. J., Saunders, A. D., Marriner, G. F. and Tarney, H. (1984). Subduction of pelagic sediments: implications for the origin Ce-anomalous basalts from the Mariana Islands. Journal of Geological Society London, 141, 453-472.